Indonesian Journal of Electrical Engineering and Computer Science
Vol. 18, No. 2, May 2020, pp. 790~798
ISSN: 2502-4752, DOI: 10.11591/ijeecs.v18.i2.pp790-798

Partial pose estimation of 3D rigid object system using outer box method

Z. Zulkoffli[1], Elmi Abu Bakar[2]
[1]Department of Mechanical and Mechatronic Engineering, UCSI University, Malaysia
[2]School of Aerospce Engineering, University Science Malaysia, Malaysia

Article Info

Article history:

Received Sep 3, 2019
Revised Nov 5, 2019
Accepted Nov 19, 2019

Keywords:

CAD/CAVI
Correlation matching
Partial pose estimation

ABSTRACT

This article introduces a novel approach for identify partial pose estimation using template matching method. The algorithms performs 2D correlation matching on tested image to CAD database by using regional shape representation in order to get the similar object pose in CAD database. The descriptor named outer box method, it is useful for rescale or aligning object size in both different images of tested image and CAD database image and also provide interest point for segmentation in image registration stage. The proposed algorithm were experimentally shown to be robust to apply on scale changes, various complex shape, unstructured CAD database and mixed CAD model database. Last part, the identified pose and its retrieved pose angle was calculated and achieved high accuracyin range ±0.388˚ to ±1.471˚.

Corresponding Author:

Zuliani Zulkoffli,
Department of Mechanical and Mechatronic Engineering,
UCSI University,
Jalan Menara Gading 1, Taman Connaught, Kuala Lumpur, Malaysia.
Email: Zuliani@ucsiuniversity.edu.my

1. INTRODUCTION

Pose estimation is a desired position and orientation of the inspected object before inspection or before robot manipulation task will take place [1]. Technological advancement on product design modelling influenced on product shape complexity [2]. Shape complexity such as free form line, almost symmetrical shape, and product features such as hole, fillet, chamfer brings difficulty on product pose estimation and inspection. This task usually done by dedicated tools, fixtures, and other part presentation devices [3]. The problem with this approach is that it takes undesirable amounts of debug and support time and is sometimes very expensive. By knowing the object pose before inspection will contributes on less time consuming for overall object inspection. External surface of whole object inspection is an essential technology operation in the production line of diverse objects [3, 4].

Although there are many methods proposed for evaluation of partial pose estimation, most of them are sensitive to noise such as shadow and insufficient object internal information especially for almost symmetrical part [2]. To address the problems, we propose a robust global shape representation using threshold binary region shape description with outer box interest point method. This outer box interest points contributes to object rescaling alignment and image registration.

Previous study presented various techniques on CAD image database development [5] using .stl data, image data acquisition for surface inspection [6], pre-processing techniques on image registration [7-18], features extraction such as Vote-based 3D shape recognition and registration [19], edges extraction [20], reflection symmetric [21], DoG-based detector presented by deriving scale-invariant mesh features for image registration [22], Local Procustes Regression (LPR) [23], Estimation-by-Completion (EbC) [24] and Customized three-dimensional template matching [25-27] has been conducted. However, issues in pose estimation was still an open problem in partial pose estimation especially for almost symmetrical shape of object.

In this paper, the study focus on object description, scaling and image registration method. The contribution of this paper two fold. First, effective scale method to align two or more source image using hypotenuse length of the outer box ratio. In this work, object scale ratio needed to overcome different size object in inspected image and CAD model image. This is important because of natural phenomena of object size where are the CCD camera placement distance influence the object size and CAD model object size influenced by the image zoom in and zoom out. Second, segmented image was using interest point of object outer box method and produced different size image. Different size segmented image was align using unique image padding used in image registration stage.

The rest of this paper is organized in four sections. Section 1 contains introduction to partial pose estimation and its related studies. Section 2 introduces methodology of the proposed partial pose estimation algorithm using outer box method. This section was divided into four steps of rescaling, image registration, correlation matching and robustness test. The Outer Box method experimental results was presented in Section 3. Comparisons with existing method was carried out in Section 3.3 and Section 4.0 summarizes the conclusions of this work.

2. RESEARCH METHODOLOGY

Development on partial pose estimation using CAD database algorithm for non contact inspection in industry was carried out. Its consists of three main contributions in processing steps which were alignment of object size scale in image, segmented image padding method in image registration stage and lastly image retrieval process.

2.1. Partial Pose Estimation Of Tested Object To CAD Database

Figure 1 shows flowchart for partial pose estimation development using CAD database. As shown in this figure, acquisited CAD image and tested image go through rescaling and image registration stage. The inspected image will retrieve the similar pose in CAD model database. Extracted object using Outer Box method was used in image segmentation before image registration stage takes place. Both sources of tested image and CAD image go through this process. Collection of CAD model images in database act as reference poses. CAD model poses for 1 degree rotation from 0 degree to 360 degree produced 360 images for ±1 degree accuracy of retrieve pose.

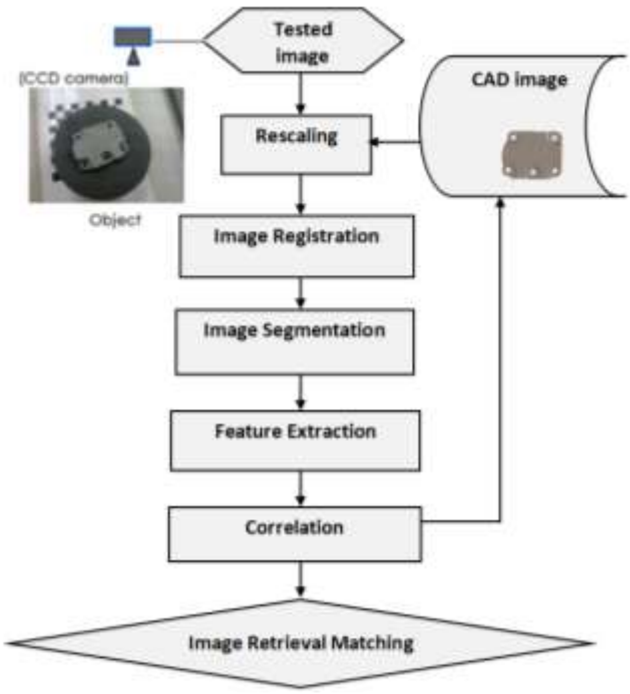

Figure 1. Flowchart representation for partial pose estimation development

2.1.1 Step 1: Outer Box For Object Size Rescaling

Hypotenuse of outer box method is a new approach for object rescaling introduced in this experiment. This method using combination of scale and rotation invariance with the local nature of object pose features. As shown in (1) and (2) were used to get salient point on outer box.

$$BoxMin = min(max(\sum_{j:I_j \geq I_p + T} |I_p - I_j| - T, \sum_{j:I_j \geq I_p + T} |I_p - I_j| - T)((\frac{\partial i, \partial j}{\partial \Delta_i, \partial \Delta_j})(i,j)) \quad (1)$$

$$BoxMax = max(max(\sum_{j:I_j \geq I_p + T} |I_p - I_j| - T, \sum_{j:I_j \geq I_p + T} |I_p - I_j| - T)((\frac{\partial i, \partial j}{\partial \Delta_i, \partial \Delta_j})(i,j)) \quad (2)$$

where I_i is intensities of pixels I, I_j is intensities of pixels j. As shown in (1) used to get coordinate of minimum point and (2) to get coordinate of maximum point of outer box. By determine that points, hypotenuse length was obtained using (3). Using this value, ratio of rescaling image size on CAD object and PRI object was calculated and applied for image processing stage.

$$c = \sqrt{(B_{imax} - A_{imin})^2 + (B_{jmax} - A_{jmin})^2} \quad (3)$$

Where B = coordinate of point B, (B_{imax}, B_{jmax}),, A = coordinate location of point A, (A_{imin}, A_{jmin}) and c = hypotenuse length of outer box method.

2.1.2 Step 2: Image Padding For Image Registration

After rescaling process, image padding in image registration process was takes place. Image registration is a stage to aligning image size for inspected image and CAD image. Image padding was using (4).

$$I_{new} = ([I_0 \; I_0 \; I_0 ; I_0 \; I \; I_0 ; I_0 \; I_0 \; I_0]) \quad (4)$$

Where I_{new} = the segmented image, I_0 = the zero padding image same size to I image and I = the extracted object image using outer box image method.

2.1.3 Step 3: Feature Extraction and Correlation Matching Retrieval

Template matching method is a technique to find similar recognize object feature in inspected image to reference image in CAD database. The basic template-matching algorithm involves sliding the template image over the source image and at each position calculating a 2D correlation of the binary image using pixel binary difference to estimate the degree of similarity between the template (CAD image) and source image (inspected image). 2D correlation in (5) was used in template-correlation matching algorithms.

$$r = \frac{\sum_m \sum_n (A_{mn} - \bar{A})(B_{mn} - \bar{B})}{\sqrt{\sum_m \sum_n (A_{mn} - \bar{A})^2 \sum_m \sum_n (B_{mn} - \bar{B})^2}} \quad (5)$$

Where A is CAD image, B is PRI image, $\bar{A}$ is mean2(A), $\bar{B}$ is mean2(B).

Figure 2 show the tested object for this partial pose estimation experiment. This figure contained, (a) automotive component (b) bottom of automotive component (c) automotive component with label (d) Arduino board (e) computer mouse and (f) USB connector. Ten test pose estimation was implemented for each object.

(a) (c) (d) (e) (f)

Figure 2. Simulation on (a) automotive component (b) bottom of automotive component (c) automotive component with label (d) Arduino board (e) computer mouse and (f) USB connector

2.2. Robustness Test

2.2.1 Step 1: Random Database

To analyse the robustness of the develop algorithm, random database structure arrangement was created in unique names. This test was performed to observe image retrieval in random CAD model database. Figure 3(a) show the image naming in CAD model file database. This test was implemented for automotive cast part in ±1 degree accuracy.

2.2.2 Step 2: Mixed Model Database

Another test was carried out in order to observe the robustness of this algorithm by mixing CAD models in CAD file database. Three trials for each object of automotive component, bottom of automotive component, Arduino board, computer mouse and USB connector were carried out. Figure 3(b) shows the CAD model image in file database.

(a) (b)

Figure 3. (a) CAD model images with unique name in file database and (b) Mixed CAD model images in file database

2.3. Accuracy Test for Partial Pose Estimation

To verify the accuracy, three reference points of Outer Box triangulation properties of test object and CAD model was calculated as in (6). The comparison angle value determined the accuracy of the propose method.

$$\theta = cos^{-1} \frac{(B_{imax} - A_{imin})}{c} \quad (6)$$

Where θ is angle error, B_{imax} is pixel *i* coordinate at point maximum of outer box and A_{imin} is pixel *i* coordinate at point minimum outer box.

3. EXPERIMENTAL RESULTS AND ANALYSIS

Figure 4 show hardware set up for inspected object image acquisition. Single CCD camera was placed at top view during image acquisition. CAD model database development using SolidWorks platform and saved into .slp file format. Using this .slp model, the CAD model rotated at z axis for image acquisition at θ interval. The *θ* was set at 1 degree rotation during image acquisition and results on structure arrangement of CAD model database.

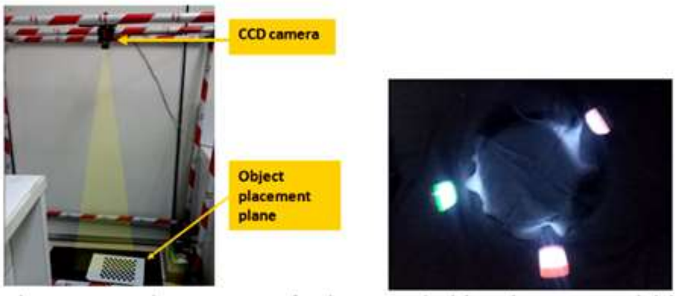

Figure 4. Hardware set up for inspected object image acquisition

3.1. Pre-Processing (Rescaling, Image Padding and Image Segmentation)

The partial pose estimation measurement system works as follows. First, the test image and CAD image go through binary image filtering at certain threshold value, this is purpose to extract the object from the background. For example, automotive component set at >30 threshold value on test image and set at >50 threshold value on CAD image. After object extraction, the outer box method applied on both object. Interest points on Outer box gives information on hypotenuse length on the test object and CAD object. Using this hypotenuse length, standard object size and CAD object size determined. However, using this outer box method, hypotenuse length varied at all different poses. In this stage, hypotenuse length ratio to CAD object and tested object was use to resize the image at standard scale. After rescaling, image size varied for both test image and CAD image. The extracted image padded with same size zero pixel image around the extracted image using (4).

Figure 5 shows the rescaling object, image padding and segmented image results for both inspected object image and CAD object image for single pose of tested objects. The image padding for inspected image was varied based on size of the inspected object outer box. The image padding for CAD image was varied on size of CAD model object outer box. Standardize image size through image registration performance was produce at a standard image size for both inspected image and CAD image.

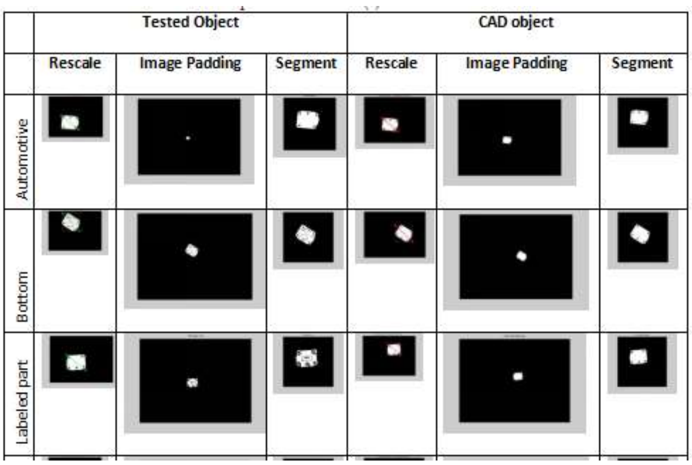

Figure 5. Extracted information on simulation object

3.2. Processing (Image Retrieval Using Correlation Matching)

Image retrieval using correlation matching of tested image to all CAD images in database. Highest correlation value determined the similar pose estimation of the tested image. Figure 6 shows the tested image and its retrieved CAD model pose in database for all tested objects. The tested object results on set of tested object together with retrieved CAD model and image retrieval graph for pose in CAD database. The graph marked with the highest peak that indicate the similar pose of tested object and CAD model pose. Table 1 indicate the average recognition rate, average processing time, average accuracy for all tested object within ten times trial at different pose. In this table, average recognition rate was varied for different object model. Various recognition rate value were caused by shape representation information on the tested object and CAD model such as corner and edge. Recognition rate value were calculated by 2D correlation matching similarity of tested object image and CAD model image, this fully beneficial in recognizing significant object area with internal shape information. Average processing time also different for different tested object model and depending on information on the image. Average accuracy obtained also showed different average accuracy on different test model. However, in overall, the accuracy fall in range ±0.83˚ to ±1.14˚ value. Planar shape component such as Bottom Automotive Component shows the highest accuracy obtained at ±0.83˚. Little shadow appearance on computer mouse slightly interrupt the image retrieval process at 81.86% recognition rate within ±1.05˚ accuracy. Different manufacturing material of USB connector shows some part of the tested object did not fully transform into binaries during image retrieval process, in this case the different of metal and plastic part did not have same value threshold. Threshold value for plastic was >30, while for metal was <5. Although partial of object information provided, this method successfully identified partial pose estimation within ±1.13˚ accuracy.

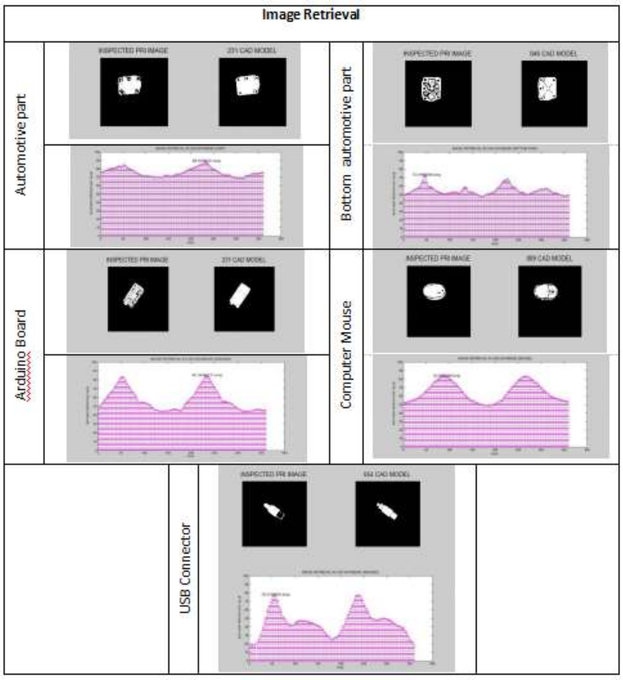

Figure 6. Correlation matching results for automotive component, bottom automotive component, Arduino board, computer mouse and USB connector

Table 1. Recognition Rate and Image Retrieval Performance of Different Type Object

Object	Average recognition rate	Average processing time (s)	Average accuracy
Automotive component	93.78 %	1009.4s	±1.14˚
Bottom automotive component	76.24%	986.0s	±0.83˚
Arduino Board	84.86%	938.2s	±1.03˚
Computer mouse	81.86%	1034.0s	±1.05˚
USB connector	84.54%	1141.8s	±1.13˚

3.3. Robustness

3.3.1 Tested Object With Labeled Noise

Figure 7 shows tested image retrieval for automotive component with label to CAD model database. Ten tests were done in this condition and achieved average retrieval accuracy at ±1.14˚ in this experiment. Table 2 shows the average recognition rate, processing time and average accuracy for this experiment. Label appearance on the tested object does not affect the effectiveness of image retrieval process, but slightly influence lower correlation value down to 7.33% on retrieved pose. Processing time taken for labelled automotive component shows increases up to 19.9s compared to non label automotive component. In Table 2, column two shows single pose image retrieval for automotive component to random structure CAD model database. Ten test were done in this condition and resulted on average accuracy at ±1.15˚ in this experiment.

Average recognition rate for random CAD database shows no significant difference compared to structure CAD database within 0.03% and no difference on average processing time. The results shows similar correlation value of pose estimation retrieved in this process compared to structure CAD model database. Random CAD model database influence all correlation graph structure and not effect on retrieval value as in Table 2.

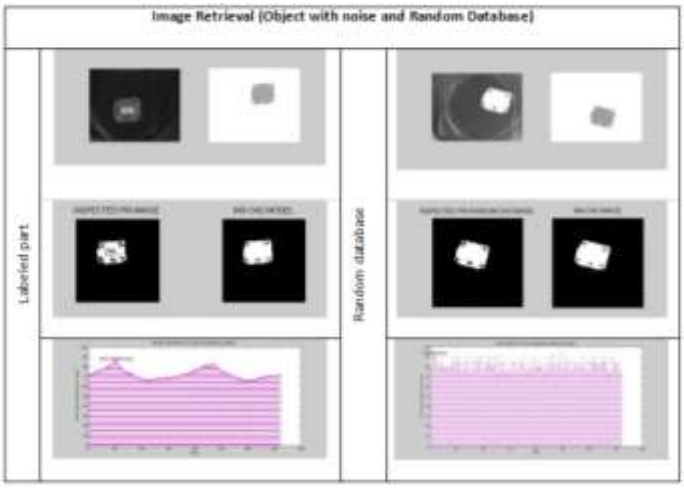

Figure 7. Image retrieval using correlation matching of automotive component at (a) labelled noise and (b) within random CAD database

Table 2. Recognition Rate and Image Retrieval Performance within Noise Information

Condition	Average Recognition rate	Processing time (s)	Average Accuracy
Labelled automotive component	86.45%	1029.3s	±1.14˚
Random arrangement database	93.75%	1009.4s	±1.15˚

3.3.2 Image Retrieval in Mixed CAD Database

Another robustness test was implemented using image retrieval in mixed CAD model database had been carried out. Three different poses were tested in this mixed CAD model database for automotive component, bottom automotive component, Arduino board, computer mouse and USB connector. Table 3 show average accuracy at ±1.14˚ for automotive component, ±0.38˚ for bottom automotive component, ±1.05˚ for Arduino board, ±1.07˚ for computer mouse and ±1.12˚ for USB connector. Average recognition rate also shows different range value for different model, which the highest for automotive component at 90.81% and the lowest for bottom automotive component at 73.34%. Average processing time varied for different model in range 464.8s to 572.9s. This processing time taken in 180 images CAD database. This proved, this feature representation is robust in mixed CAD model database.

Table 3. Recognition Rate and Image Retrieval Performance in Mixed CAD Model Database

Mixed model database	Average Recognition rate	Average Processing time (s)	Average Accuracy
Automotive component	90.81%	477.8s	±1.14˚
Bottom automotive component	73.34%	551.8s	±0.38˚
Arduino Board	81.57%	464.8s	±1.05˚
Computer mouse	88.32%	516.7s	±1.07˚
USB connector	75.55%	572.9s	±1.12˚

3.4. Comparisons With Existing Method

Table 4 shows comparison accuracy result of the proposed method and previous study. In this table, this presented work shows a highly competitive results on accuracy in this partial pose estimation identification of tested object to CAD model database within range ±0.388˚ to ±1.471˚ error. Naoki et. al [28], Carlos et. al [8] and Toshiyuki & Toru [26] development obtained pose estimation error at ±5.81, ±1.50 to ±4.84 and ±2.26 to ±2.07 degrees, respectively.

Table 4. Comparison of Propose Method to Previous Study

Method	Accuracy (degree)
Outer Box Correlation Matching	±0.38˚ to ±1.47˚
Naoki et. al [28]	±5.81˚
Carlos et. al [8]	±1.50˚ to ±4.84˚
Toshiyuki & Toru [26]	±2.26 to ± 2.07

4. CONCLUSIONS

In this paper, a novel approach for partial pose estimation identification was introduced that using geometric information from CAD models. This work was successfully able to combine the appearance information of tested object to CAD models image. Notably, our algorithm outperforms on accuracy and introduced feature robustness, and significantly improves existed method on partial pose estimation identification. We believe that our work provides a platform to tackle higher level tasks such as 3D pose estimation identification and multi view image registration.

ACKNOWLEDGEMENTS

The authors would like to be obliged to Malaysia Ministry of Higher Education for MyBrain15 sponsorship.

REFERENCES

[1] C. Zang, and K. Hashimoto, *"A flexible visual inspection system combining pose estimation and visual servo approaches,"* IEEE International Conference on Robotics and Automation, River Centre, Saint Paul, Minnesota, 2012, pp. 1304 - 1309.

[2] S. Kwon et al, "Feature shape complexity: a new criterion for the simplification of feature-based 3D CAD models," *The International Journal of Advanced Manufacturing Technology*, vol 88, pp. 1831–1843, 2017.

[3] P. Griffin et al, "Process Capability of Automated Visual Inspection Systems," I*EEE Transactions On Systems, Man, And Cybernetics*, vol. 3(22), pp. 441-448, 1992.

[4] A. Bondarevskii et al, " Metrological Service : Determination Of Metrological Performance Of Visual Inspection Operators," *Measurement*, vol. 2(43), pp. 182-188, 2000.

[5] F. A. Adnan et al, *"Real-time slicing algorithm for Stereolithography (STL) CAD model applied in additive manufacturing industry"*, IOP Conf. Ser.: Mater. Sci. Eng. Vol. 3(42) pp. 012-016, 2018.

[6] C. Banica et al, "Data acquisition and image processing system for surface inspection," *10th International Symposium on Advanced Topics in Electrical Engineering (ATEE)*, Bucharest, 2017, pp. 28-33.

[7] B. Bajić et al, "Sparsity promoting super-resolution coverage segmentation by linear unmixing in presence of blur and noise," *Journal of Electronic Imaging (SPIE),* vol. 28(1), pp. 013-046, 2019.

[8] T. Carlos et al, "3D point cloud registration based on a purpose-designed similarity measure," *EURASIP Journal on Advances in Signal Processing*, vol. 2(57), pp. 1680-1687, 2012.

[9] J. Cougoung et al, "An effective approach for point clouds registration based on the hard and soft assignment," *Journal of Photogrammetry and Remote Sensing,* vol. 1(3), pp.124-138, 2017.

[10] Lu, Yan et al. "A novel image registration approach via combining local features and geometric invariants," *PloS one* (2018).

[11] D. Paquin et al, "Multiscale Image Registration," *Mathematical Biosciences and Engineering,* vol.3(3), pp. 389-418, 2006.

[12] E. Chen et al, "A Novel Multiscale Edge Detection Approach Based on Non subsampled Contourlet Transform and Edge Tracking," *Mathematical Problems in Engineering,* vol. 1, pp. 1-14, 2015.

[13] J.Öfverstedt et al, "Fast and Robust Symmetric Image Registration Based on Distances Combining Intensity and Spatial Information," *IEEE Transactions on Image Processing*, vol. 28(7), pp. 3584-3597, 2019.

[14] L. Xiaolong et al, "Recent progress in semantic image segmentation," *Artificial Intelligence Review,* vol. 52(1), pp. 1089-1106, 2019.

[15] X. Zheng et al, "Image segmentation based on adaptive K-means algorithm," *EURASIP Journal on Image and Video Processing,* vol. 68(1), pp. 1-6, 2018.

[16] K. Li et al, "A course-to-fine registration strategy for multi-sensor images with large resolution differences," *Remote sens,* vol. 11(1), pp. 470-475, 2019.

[17] Q. Jiang et al, "Multi-Sensor Image Fusion Based on Interval Type-2 Fuzzy Sets and Regional Features in Nonsubsampled Shearlet Transform Domain," *IEEE Sensors Journal*, vol. 18(6), pp. 2494–2505, 2018.

[18] J. Chen, and L. Li, "Segmentation of Microlens Surfaces Based on Contourlet Transform and Mathematical Morphology," *Semiconductor Optoelectronics*, vol. 38(6), pp. 839–843, 2017.

[19] Y. Xiang et al, "An Automatic and Novel SAR Image Registration Algorithm: A Case Study of the Chinese GF-3 Satellite," *Sensors,* vol. 18(2), pp. 672-678, 2018.

[20] P. Minh-Tri et al, "Scale-Invariant Vote-Based 3D Recognition and Registration from Point Clouds," R. Cipolla et al. (Eds.) Chapter in book Machine Learning for Computer Vision, SCI 411, pp. 137–162, 2012.

[21] E. Dong et al, *"FPGA Based Design and Implementation of Improved Edge Detection Algorithm using LOG Operator,"* IEEE International Conference on Mechatronics and Automation (ICMA), 2018, pp. 2092–2096,
[22] W. Cheng-Hei et al, *"CAD-Based Pose Estimation for Random Bin-Picking of Multiple Objects Using a RGB-D Camera,"* 15th International Conference on Control, Automation and Systems (ICCA 2015), BEXCO, Busan, Korea. 2015, pp. 1645- 1649.
[23] B. Ehud and B. Ohad, "Depth Based Object Detection from Partial Pose Estimation of Symmetric Objects". D. Fleet et al. (Eds.) Chapter in book ECCV Part V, LNCS 8693, pp. 377–390, 2014.
[24] D. Tal, D and K. Yosi, "Scale-Invariant Features for 3-D Mesh Models," *IEEE Transactions On Image Processing*, vol. 5(21), pp. 2758- 2769, 2012.
[25] R. Bisser et al, "*Object Pose Estimation by Locally Linearly Embedded Regression*" 18th IEEE International Conference on Image Processing, 2011, pp. 3585- 3588.
[26] A. Toshiyuki et al, *"An Appearance Based Fast Linear Pose Estimation,"* MVA2009 IAPR Conference on Machine Vision Applications, May 22, Yokohama, Japan, 2009, pp. 182- 186.
[27] O. Roberto et al, "A Model- Based 3D Template Matching Technique for Pose Acquisition of an Uncooperative Space Object," *Sensors*, vol.15, pp. 6360-6382, 2015.
[28] K. Naoki et al, *"Three-DoF Pose Estimation of Asteroids by Appearance-based Linear Regression with Divided Parameter Space,"* MVA2015 IAPR International Conference on Machine Vision Applications, May 18-22, Tokyo, Japan, 2015, pp. 14-33.

BIOGRAPHIES OF AUTHORS

Zuliani binti Zulkoffli is currently lecturer at UCSI University, Kuala Lumpur. She's obtained her postgraduate certificate from Universiti Sains Malaysia on CAD/CAM field through image processing method. Her master certificate was in Material Science in mechanical Engineering from Universiti Kebangsaan Malaysia. Her deep interest to explore paved a way to understand on multiple view analysis. Other interest also in instrumentation, material science and manufacturing.

Elmi Abu Bakar is currently Associate Professor in University Science Malaysia, USM. He's obtained all his higher educations certificates from Japan starting by his Dip. Eng Mechanical at Kisarazu, Bachelor Engineering Mechanical at Iwate, Master Engineering Production System at Toyohashi and last but not least his PhD certificates in Electronics and Information at Toyohashi, Japan. His research interests on Machine Vision (Image based Measurement), Control System and Robotics (WMR), Abnormal detection using Signal Processing Methods, Shape Classification and Analysis, CAD,Tool & Die Quality Inspection and Computer Aided Inspection.